Effect of low temperature synthesis of carbon nanotube nanocomposite on the photovoltaic performance of anode buffer layer in polymer solar cells

IOP Conf. Series: Materials Science and Engineering **805** (2020) 012026 doi:10.1088/1757-899X/805/1/012026

Effect of low temperature synthesis of carbon nanotube nanocomposite on the photovoltaic performance of anode buffer layer in polymer solar cells

H O Oyeshola[1], M A Adisa[2,3], B K Adejumo[1], K K Babalola[1], B A Agboluaje[1], O Adedokun*[1,4] and Y K Sanusi[1,4]

[1]Department of Pure and Applied Physics, Ladoke Akintola University of Technology, Ogbomoso, Oyo State, Nigeria.

[2]Department of Physics and Material Science, Kwara State University, Malete, Kwara State, Nigeria.

[3]Rubber Research Institute of Nigeria, Benin City, Edo State, Nigeria.

[4]Nanotechnology Research Group (*NANO*$^{+}$), Ladoke Akintola University of Technology, Ogbomoso, Oyo State, Nigeria.

*Email: oadedokun@lautech.edu.ng; adedokunoluwaseun2@gmail.com

Abstract

Today's solar cells are simply not efficient enough and are currently too expensive to manufacture for large-scale electricity generation. However, potential advancements in nanotechnology may open the door to the production of cheaper and slightly more efficient solar cells. This research is based on the study of photovoltaic properties of low temperature synthesized carbon nanotube (CNT) nanocomposite as an anode buffer layer for the PEDOT:PSS based polymer solar cells. CNT was synthesized using simple and cost effective method at low temperature. The structural and optical properties of prepared CNT samples were characterized using X-ray diffraction (XRD) analysis, Fourier Transform Infrared (FTIR) spectroscopy, Scanning Electron Microscopy (SEM) and UV spectroscopy. CNT/PEDOT:PSS nanocomposite solutions was prepared and spin coated on a cleaned glass substrate at different spin coating speed, the fabricated buffer layer thin film devices were annealed from 100 ˚C to 500 ˚C, their optical and electrical properties were then analyzed. The XRD of synthesized CNTs nanoparticles show diffraction pattern which exhibit tetragonal structure and FTIR shows functional group of carbon nanotube. The SEM image showed that the obtained sample

maintained tubular structure, cluster at 20 nm but properly dispersed at 100 nm. The optical studies of the films show an increase in absorbance as the annealing temperature increases. The photovoltaic performance of the polymer solar cell showed an improved efficiency of 6.44 % for optimized device. It is deduced from this work that low temperature synthesized CNT nanocomposite demonstrated better performance as anode buffer layer for high efficient polymer solar cells.

Keywords: Polymer solar cells; CNT; PEDOT:PSS; nanocomposite, anode buffer layer

1 Introduction

The branch of technology that studies different materials at a nanometric scale is referred to as nanotechnology and it is also defined as science of production, manipulation and use of materials at subatomic level that finds its application in various disciplines [1]. There is increasing global interest in alternative forms of energy, sunlight is a particularly promising clean and readily available source compared with conventional fossil fuels. Solar cells are devices that directly convert solar energy into electricity [2-3]. Nowadays, the processing methods for fabricating devices become increasingly more complex, resulting in higher production costs. Beside the high cost that limits the range of applications in daily life; poor mechanical flexibility also limits use in applications requiring flexible substrates. Organic-based electronic devices have a promising future despite their lower performance as semiconductors because of several unique properties of organic materials. However, the realization of large-scale organic solar cells is slowed because of their poor environmental stability and charge transport across the photoactive medium.

Introduction of carbon nanotubes (CNTs) into the photoactive layers of organic photovoltaic (OPV) cells were intended to mitigate shortcomings of conjugated polymer solar cells. Photovoltaic (PVs) can be rolled out onto a roof or other surfaces, and they are less prone to damage and failure than traditional solar cells. Being organic, polymer PVs are also more environmentally friendly [4-6]. CNTs and conjugated polymers have a similar sp2 type hybridization and exhibit high electrical conductivity [7]. However, even though CNTs have shown potential in the buffer layer, they have not resulted in a solar cell with power conversion efficiency greater than the best tandem organic cells (6.5% efficiency). But, it has been shown in most of the previous investigations that the control over a uniform blending of the electron

donating conjugated polymer and the electron accepting CNT is one of the most difficult as well as crucial aspects in creating efficient photocurrent collection in CNT-based OPV devices. Therefore, using CNTs as buffer layer in OPV devices is still in the initial research stages and there is still room for novel methods to better take advantage of the beneficial properties of CNTs. In this research, CNT was synthesized at low temperature using simple and cost effective method; the synthesized CNTs were then incorporated into PEDOT:PSS to modify anode buffer layer for the overall efficiency improvement of OPV.

2. Experimental details

2.1 Chemicals and materials

The materials used are graphite powder, nitric acid, sulphuric acid, potassium chlorate, poly (3,4-ethylene dioxythiophene): poly (styrene sulfonate) (PEDOT:PSS), distilled water, ethanol, acetone, isopropanol alcohol (IPA), glass substrates, and FTO coated glass.

2.2 Synthesis of carbon nanotube (CNT)

The graphite powder of 5 g was slowly added to the mixture of 25 ml of nitric acid and 50 ml of sulfuric acid for 30 min. The mixture was later cooled to 5 ^{o}C in ice bath. Then, 25 g of potassium chlorate was added to the above solution under continuous stirring for 30 min leading to the evolvement of heat. After that, the solutions were then placed in air for three days; after the three days, graphite precipitates were at the bottom while the carbon floated. The floating carbon material was transferred into distilled water (1 litre) for purification. After stirring it for one hour, the solution was immediately filtered and the sample was dried. The process was repeated four times.

2.2.1 Characterization of synthesized CNTs

Synthesized CNTs were characterized to investigate the chemical and structural properties using FTIR (BUK, lnfrared spectrophotometer model M530), SEM (ASPEX 3020) and XRD PANalytical system diffractometer (DY-1656), respectively.

2.3 Substrate preparation

All experimental procedures for the preparation of the thin films were performed under ambient air. Clean rectangular glass slides of dimension 25.4 mm by 76.2 mm were used as substrates. The glass substrates were washed with detergent solution for 10 to 15 min in ultrasonicator and rinsed in distilled water for 15 min at 30˚C. The substrate was cleaned with isopropanol alcohol in ultrasonic bath for 15 min at 30 ˚C and dried in a stream of nitrogen gas (N_2).

2.4 Deposition of anode buffer layer thin film devices

The solutions of CNT/PEDOT:PSS nanocomposites were prepared and deposited on glass substrate at different spin-coating speed using spin-coater machine (Laurel WS-650Hz-23NPP). Spin coating speeds of 3000, 2000 and 1000 rpm were considered respectively for 30 seconds corresponding to thin film layer thicknesses of 32, 35, and 115 nm respectively. Depending on the speed of rotation (rpm) of the spin coater, the desirable thickness of the sample was obtained. It is important to note that the thickness of film being spin -coated depend on both time and speed of rotating stub as specified by equipment manufacturer in absence of surface profilometer.

2.4.1 Optical characterization of anode thin film devices

Optical characterization of thin film sample was carried out using UV-vis spectrophotometer (Avantes Avalight-DH-5-BAL). The photocurrent (current–voltage) of CNT/PEDOT:PSS buffer layer thin films devices were measured under simulated illumination at AM 1.5 G, 100 mW/cm^2 with a Keithley 2400 source meter. The wavelength spectrum for which a material absorbs light and produces photocurrent helps determine whether the material is capable of converting the available light illuminating it into electric energy. Absorption was chosen as the optimization variable because the choice of layer thickness is critical for optimization of the efficiency. UV-vis spectrophotometer was used to record the transmittance and reflectance in percentage (%). Absorbance was calculated using Equation (1) and (2) respectively [12].

$$A + R + T = 1 \quad (1)$$

$$\text{Absorbance (A)} = 2 - \log 10(\%T) \quad (2)$$

2.4.2 Photovoltaic properties of thin films devices

The current- voltage characteristics of thin films were carried out under illumination of solar simulator with Keithley source meter (2400 SMU). The short-circuit current (I_{SC}) and open-circuit voltage (V_{OC}) were recorded using equation (3) and (4).

$$FF = \frac{J_m \times V_m}{J_{sc} \times V_{oc}} \quad (3)$$

$$\eta = \frac{P_{out}}{P_{in}} = \frac{J_{sc}.V_{oc}.FF}{P_{in}} \quad (4)$$

3.0 Results and Discussion

3.1 Scanning electron microscope (SEM) images of synthesized CNTs nanoparticles

Studies of the morphology of the synthesized nanoparticles showed that the obtained sample maintained their tubular structure at the origin of their strength. The obtained dried samples at 20 nm are cluster to each other but at 100 nm it shows properly dispersed nanotubes as indicated in Figures 1(a) and 1(b) respectively. The closely contacting interface between them is vital for the separation of electron hole pairs and the transportation of electron and holes, which are important for the hybrid solar cells to obtain high performance in agreement with reports in the literature [13-15].

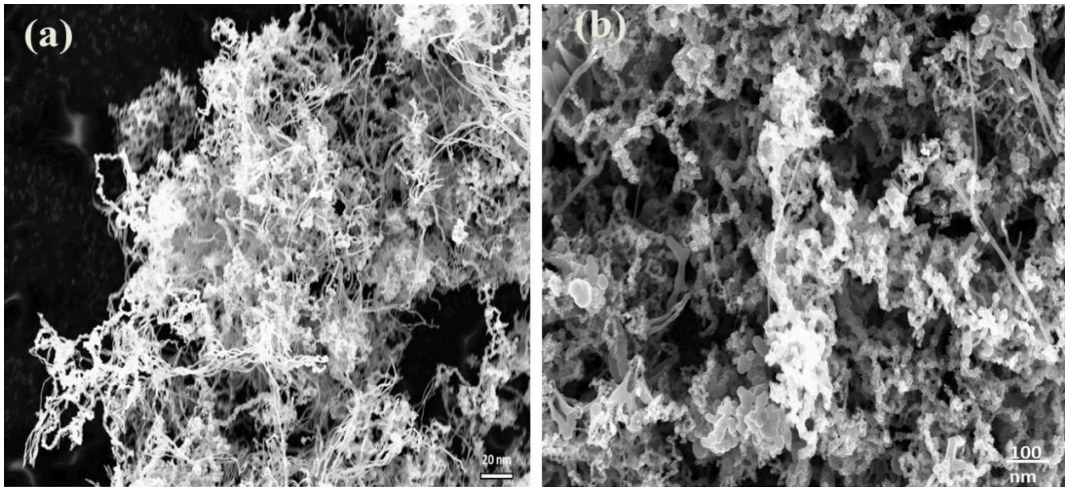

Figure 1. SEM images of (a) CNT at 20 nm (b) CNT at100 nm

3.2 X-ray diffraction (XRD) of synthesized CNTs nanoparticles

Figure 2 shows the XRD analysis of synthesized CNTs. The pattern exhibited the diffraction peaks of (002) and (100) plane of the carbon nanotube. The tetragonal structure of carbon nanotube was confirmed and the value of the lattice constants was in good agreement with the standard JCPDS value as shown in Figure 2

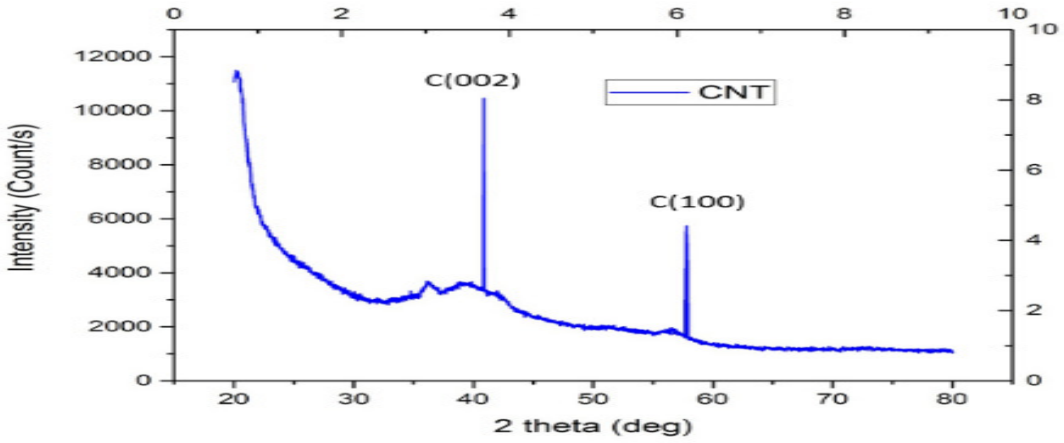

Figure 2. The XRD pattern of synthesized CNTs

3.3 Fourier transform infrared (FTIR) of synthesized CNTs analysis

FTIR spectrum of synthesized CNTs is shown in Figure 3 and was recorded in the range of 4000 to 500 cm^{-1}. It was observed that the band of synthesized CNTs occurs at 3632.98, 3419.89, 1633.79, 1384.27, 1224.71, 1064.69, 1020.41, 963.55, 850.3, 725.25, 623.69, 495.50 and 445.0 cm^{-1}. The strong band at 445 cm^{-1} is ascribed to the N-H, C-H bending mode and the signal at 495.50 cm^{-1} and 963.55cm^{-1} are ascribed to the C-H vibration bands in the synthesized CNT. The adsorption peaks at 1633.97 cm^{-1} and 1020.41 cm^{-1} correspond to the stretching modes of the C=O bond of the carbonic groups. These results show that synthesized CNT have been prepared successfully as reported by earlier workers [7, 11, 16-20].

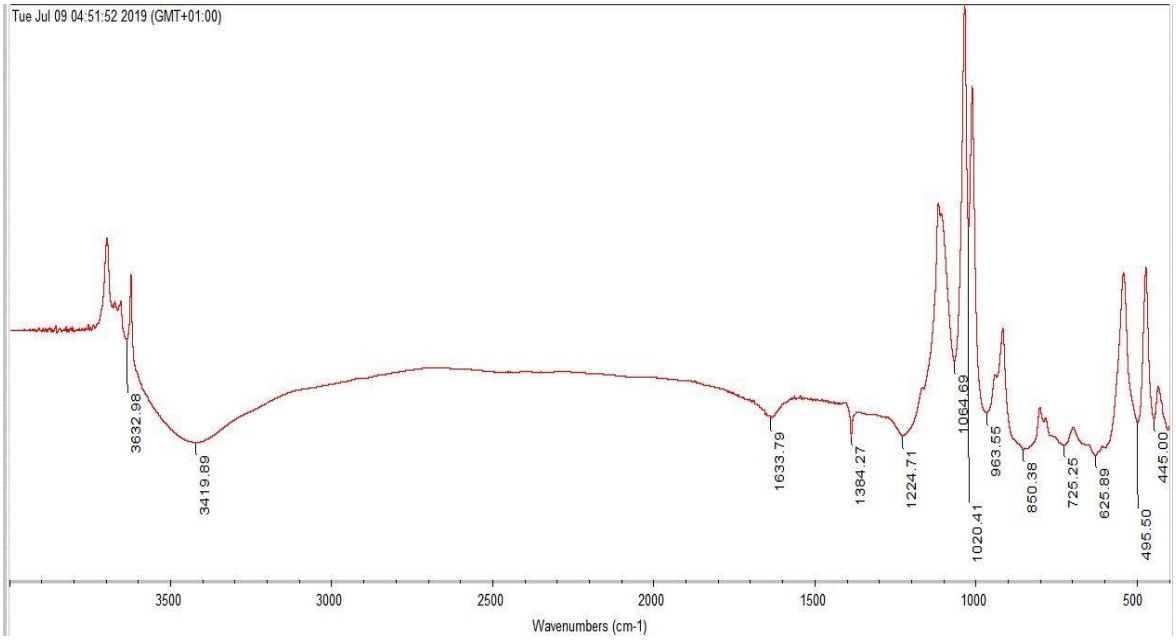

Figure 3. FTIR spectrum of synthesized CNTs

3.4 Optical characteristics of film devices at different speeds

The optical absorbance was calculated using equation 2. Figure 4 shows the absorbance graph of thin film devices spin coated at different spin coating speed using acetone as the solvent. It was observed that as the wavelength increases there is an increase in absorption; this displays the effects of the CNTs nanoparticles on the light absorption and charge separation efficiency of the conjugated polymer buffer layers. UV-visible absorption was measured for 1000, 2000 and 3000 rpm respectively deposited on glass substrates. It was observed from the graph that the highest absorbance value was at 2000 rpm and the least value was at 3000 rpm.

3.5 Optical characteristics of film devices at different annealing temperatures

The absorbance spectra of film devices were annealed at temperature range from 100 to 500 °C with a step of 100 °C. The maximum absorbance was at 200^{o} C and estimated using equation 2, least value was at 400 ^{o}C as shown Figure 5. There is an increase in absorbance as the

wavelength increases; this could be due to structural homogeneity, crystallinity and the thicknesses of films, as reported by other researches [9, 21]. It was observed from the graph that the sample annealed at 400 ^{o}C has the highest value of absorbance.

3.6 Photovoltaic Properties of Thin Films Devices

Figure 6 shows the I-V measurement under solar simulation for optimized device. The fill-factor (FF) and efficiency (η) were calculated using equations (3) and (4), respectively. After the optimization of the parameters, the best rotating speed and annealing condition of anode buffer layer thin film device were determined and also the effect of annealing time on the performance of this devices were also investigated. Therefore, the device with annealing temperature of 400 ˚C at 30 min shows a slightly higher performance compared to others shown in table 1, this improvement can be ascribed to the enhancement of the absorption intensity of the device, increased defects in the hole transport layer that act as recombination centers to improve the conductivity. The optimized fabricated CNT/PEDOT:PSS anode buffer layer thin film device under illumination has the efficiency of 6.44%.

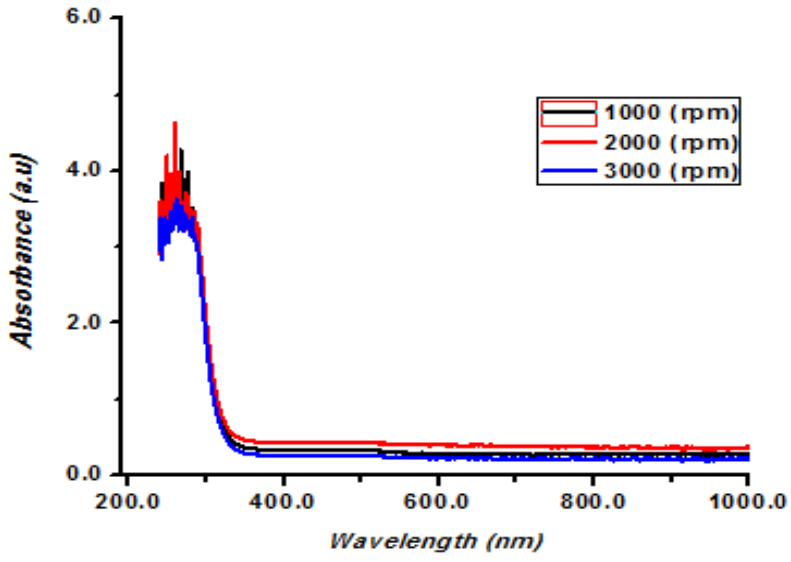

Figure 4. Optical absorbance spectra of film devices at different spin speed (rpm)

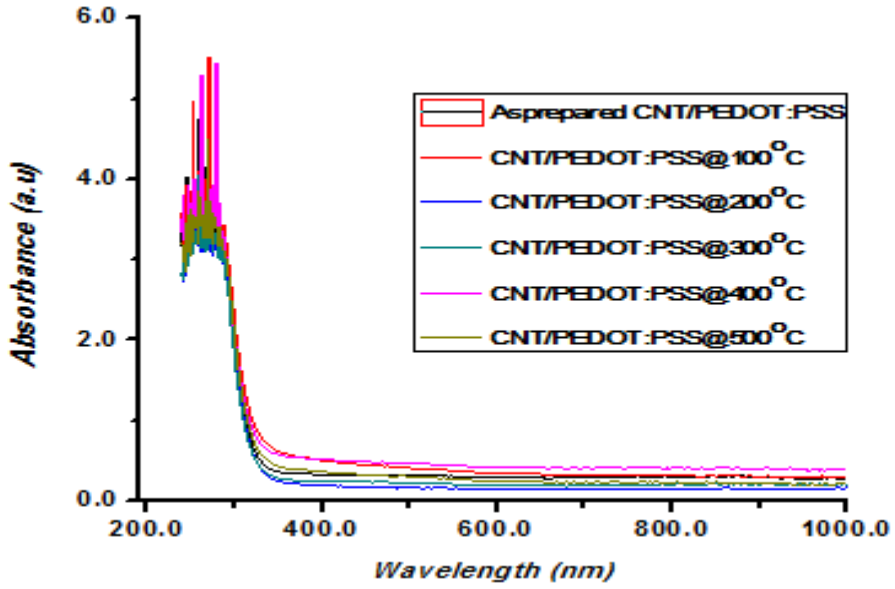

Figure 5. Optical absorbance spectra of film devices at different annealing temperatures

Table 1. Summary of photovoltaic parameter for the optimized anode buffer layer thin film devices

CNT/PEDOT:PSS (rpm)	Annealing (°C)	Time	V_{OC} (V)	J_{SC} (mA/cm^2)	P_{MAX} (W)	FF (%)	Efficiency (%)
2000	400	1 h	0.60	10.54	6.324	66	5.78
2000	400	30 min	0.72	11.02	7.934	72	6.44
2000	400	15 min	0.71	10.68	7.583	67	5.80

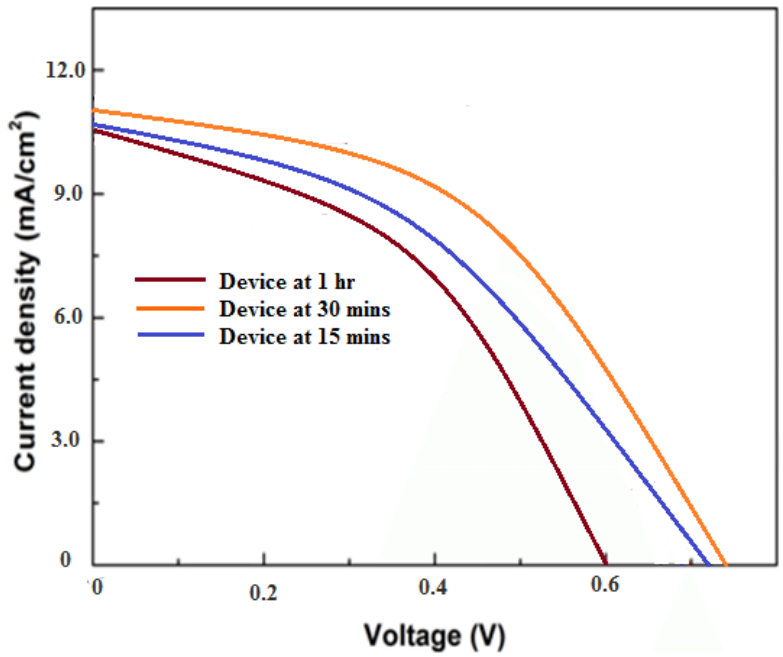

Figure 6. Current voltage curve of optimized CNT/PEDOT:PSS Thin Film Devices

4 Conclusion

This research focused on the synthesis of CNTs using a simple and cost effective method. The structural and electrical characterization was carried-out by using SEM, XRD, FTIR and Kiethley source meter, respectively. Optimization of optical properties was done using UV-vis Spectrophotometer. The synthesized CNTs were incorporated into polymer materials **(**PEDOT:PSS) anode buffer layer and the impact of post thermal annealing was investigated. It can be concluded that optimized spin coating speed and annealing condition increased the optical properties of the devices so as to enhance the performance of polymer solar cells. The photovoltaic performance evaluation of the polymer solar cells showed that open circuit voltage (Voc) ranged from 0.60 to 0.72 V and short circuit current density (Jsc) was in the range of 10.54 to 11.02 $mAcm^{-2}$. The improved efficiency of 6.44 % was recorded for device annealed for 30 min which enhance faster travelling of holes to the anode.

References

[1] Siddiki MK, Li J, Galipeau D and Qiao Q 2010 A review of polymer multijunction solar cells. *Energ. Environ. Sci.* **3** (7) pp 867-883.

[2] Baluschev S, Nelles G, Landfester K and Miteva T 2012 Sun-light up conversion in multi-component organic systems: development towards application for solar cells outcome enhancement. *Next Generation (Nano) Photonic and Cell Technologies for Solar Energy Conversion III* **8471** 84710E. https://doi.org/10.1117/12.928929.

[3] Kroon R, Lenes M, Hummelen JC, Blom PW and De Boer B 2008 Small bandgap polymers for organic solar cells (polymer material development in the last 5 years). *Polym. Rev*. **48** (3) pp 531-582.

[4] Said E 2009 Electrolyte Semiconductor Combinations for Organic Electronic Devices. Linköping University: Studies in Science and Technology. Doctoral Dissertations, No. **1228** *ISBN: 978-91-7393-735-1*.

[5] Anokhin DV, Gerasimov KL, Kiriy A and Ivanov DA 2015 Thermal annealing effect on active layer structure in all-polymer organic solar cells. *Appl. Mech. Mater.* **792** pp. 640-644.

[6] Frohne H, Shaheen SE, Brabec CJ, Müller DC, Sariciftci NS and Meerholz K 2002 Influence of the anodic work function on the performance of organic solar cells. *Chem. Phys. Chem*. **3** (9) pp 795-799.

[7] Liang F, Shi F, Fu Y, Wang L, Zhang X, Xie Z and Su Z 2010 Donor–acceptor conjugates-functionalized zinc phthalocyanine: Towards broad absorption and application in organic solar cells. *Sol. Energ. Mater. Sol. Cells* **94** (10) pp 1803-1808.

[8] Shi H, Liu C, Xu J, Song H, Lu B, Jiang F, Zhou W, Zhang G and Jiang Q 2013 Facile fabrication of PEDOT: PSS/polythiophenes bilayered nanofilms on pure organic electrodes and their thermoelectric performance. *ACS Appl. Mater. Interf.* **5** (24) pp 12811-12819.

[9] Alturaif HA, ALOthman ZA, Shapter JG and Wabaidur SM 2014 Use of carbon nanotubes (CNTs) with polymers in solar cells. *Mol.* **19** (11)17329-17344.

[10] Lin JS, Chu WP, Juang FS, Chen NP, Tsai YS, Chen CC, Chen CM and Liu LC 2012 Manufacture of light-trapping (LT) films by ultraviolet (UV) irradiation and their applications for polymer solar cells (PSCs). *Mater. Lett*. **67** (1) pp 42-45.

[11] Nguyen TL, Lee TH, Gautam B, Park SY, Gundogdu K, Kim JY, Woo HY. Single component organic solar cells based on oligothiophene-fullerene conjugate. *Adv. Funct. Mater.* **27** (39)1702474. https://doi.org/10.1002/adfm.201702474.

[12] You J, Dou L, Yoshimura K, Kato T, Ohya K, Moriarty T, Emery K, Chen CC, Gao J, Li G and Yang Y 2013 A polymer tandem solar cell with 10.6% power conversion efficiency. *Nature Comm*. **4** 1446. https://doi.org/10.1038/ncomms2411.

[13] Gusain A, Faria RM and Miranda PB 2019 Polymer Solar Cells—Interfacial Processes Related to Performance Issues. *Front. Chem.* **7** 61. https://doi.org.10.3389/fchem.2019.00061.

[14] Nardes AM, Janssen RA and Kemerink M 2008 A morphological model for the solvent-enhanced conductivity of PEDOT: PSS thin films. *Adv. Funct. Mater*. **18** (6) pp 865-871.

[15] Kan B, Li M, Zhang Q, Liu F, Wan X, Wang Y, Ni W, Long G, Yang X, Feng H and Zuo Y 2015 A series of simple oligomer-like small molecules based on oligothiophenes for solution-processed solar cells with high efficiency. *J. Am. Chem. Soc*. **137** (11) pp 3886-3893.

[16] Awodugba A O, Sanusi Y K and Ajayi I O 2013 Photovoltaic solar cell simulation of Shockley diode parameter in Matlab. *Int. J. Phys. Sci.* **8** (22) pp 1193-1200.

[17] Bakar N A, Supangat K and Sulaiman F 2014 Controlling the morphological structural and optical properties of one-dimensional PCDTBT nanotubes by template wetting *Nanoscale Res. Lett.* **9** 600. https://doi.org/10.1186/1556-276X-9-600.

[18] Bencharrats, F., Zitouni, K., and Gil B 2010 Determination of piezo electric and spontaneous polarization fields in Quantum wells grown along the polar (0001) direction *Superlattices Microst.* **47** (5) pp 592-596.

[19] Bernamache S, Rahal A and Benhaoua B 2014 The effects of solvent nature on spray-deposited ZnO thin film prepared from Zn $(CH_3COO)_2$ $2H_2O$. *Opt.* **125** (2) pp 663-666.

[20] Bertho S, Haeldermans I, Swinnen A, Moons W, Martens T, Lusen L, Vanderzande D, Manca J, Scenes A and Bonfiglio A 2007 Influence of thermal ageing on the stability of polymer bulk heterojunction solar cells. *Sol. Eng. Mat. Sol. Cells* **91** (5) pp 385-389.

[21] Balogun S W, Sanusi Y K and Aina A O 2018 Structural and optical properties of Titanium dioxide thin film deposited by spin coating technique. *Int. J. Dev. Res.* **08** (01) pp 18486-18490.